Earth and Planetary Science Letters, 70 (1984) 303–310
Elsevier Science Publishers B.V., Amsterdam – Printed in The Netherlands

Primary differences in oxygen fugacity and depth of melting in the mantle source regions for oceanic basalts

L.V. Dmitriev [1], A.V. Sobolev [1], A.V. Uchanov [1], T.V. Malysheva [1] and W.G. Melson [2]

[1] *Vernadsky Institute of Geochemistry, U.S.S.R. Academy of Sciences, Moscow (U.S.S.R.)*
[2] *Smithsonian Institution, Washington, DC 20560 (U.S.A.)*

Received June 23, 1982
Revised version received June 18, 1984

Most abyssal basalt can be divided into two groups based on major and minor element compositions of the glassy rinds of pillow lavas. Crystal differentiation models cannot relate one group to the other. Instead, depth of partial melting may exert the primary control. The first group (MORB-1) is characterized by low TiO_2 and Na_2O and higher MgO, and is derived from a primary melt originating from the spinel peridotite facies. The higher TiO_2-NaO_2 group (MORB-2) appears to have been derived from the lower-pressure (shallower depth) plagioclase peridotite facies. Mössbauer spectra show that MORB-1 is from a mantle source region with lower oxidation states (between the QFM and NNO buffers) than for MORB-2 (around the NNO buffer).

1. Introduction

Shido and Miyashiro [1] first noted systematic differences in the composition of mid-ocean ridge basalt (MORB) from the southern and northern parts of the North Atlantic. Various models involving lateral heterogeneity of the mantle source regions, variable degrees of mantle partial melting, and magma mixing have been proposed (e.g. [2–5]) to explain this difference, as well as models involving differences in tectonic environment of melting [6–8].

A statistical study of the compositions of quenched abyssal tholeiite glasses from the world ocean shows the existence of two wide-spread compositional groups of MORB [9–13] (Fig. 1). An eight-component discriminant function was calculated to define MORB-1 (low Na_2O and TiO_2, high MgO) and MORB-2 (high Na_2O and TiO_2) glasses with 95% accuracy [13,14]. A statistical study of MORB phenocrysts shows that MORB-1 liquidus phases include $Fo_{91.5}$ and chromium spinel, while those of MORB-2 include Fo_{90}, An_{88} and chromium spinel [15,16]. It has been shown that MORB-1 has a relatively high content of siderophile-group trace elements while MORB-2 has a higher content of lithophile-group trace elements. Also, MORB-2 statistically is found to be depleted in light rare earth elements (LREE) while MORB-1 is characterized by a complex spectra of REE [2,4,17].

Some geographic regularities of MORB-1 and MORB-2 distribution have been noted [9–13,16]. For example, MORB-1 probably forms most of layer 2 of the ocean crust. Data on the Red Sea show that MORB-1 appears at the initial period of this ocean opening [17]. MORB-2 appears predominantly during the last 10–20 m.y. in the axial parts of mid-ocean ridges and in the young parts of marginal seas [16].

0012-821X/84/$03.00

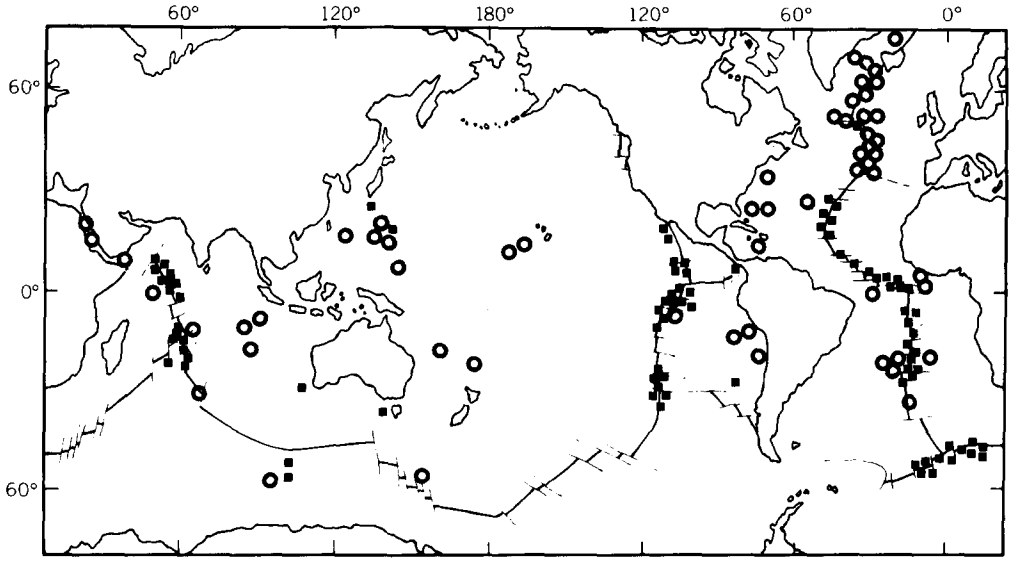

Fig. 1. Schematic map of the world ocean [16]. Data on the abyssal glass composition extracted from Melson et al. [25] and from Smithsonian collection unpublished data. ○ = glass of MORB-1; ■ = glass of MORB-2.

These data have led us to believe that MORB-1 and MORB-2 are the products of two independent primary melts. Detailed petrological investigations have further developed this idea and involve the use of recent experimental petrologic data [18–24], melt microinclusions in MORB phenocrysts, and the use of mathematical models of crystal fractionation. We infer that MORB-1 is the product of near-surface differentiation of a high-magnesian (MgO ~ 14% wt.%) primary melt probably originating from dry spinel lherzolite at $T \sim$ 1350 °C and $P = 10$–15 kbar. MORB-2 is inferred

TABLE 1

Localities for samples described in Table 2

Location No.	Locality description			Analysis No.
1	MAR	36.80 °N, 33.27 °W	Alvin 504-2	(VG 3424)
2	MAR	36.81 °N, 33.27 °W	Alvin 525-2	(VG 3393)
3	MAR	36.66 °N, 33.34 °W	Knorr 42, St 86, Dr 12	(VG 3269)
4	MAR	36.72 °N, 33.33 °W	Atlantis II 77, St 37, Dr 6	(VG 3321)
5	MAR	40.30 °N, 29.28 °W	Kurchatov 6, St. 402	(432-2-1)
6	MAR	37.30 °N, 35.20 °W	DSDP Site 335	(VG 2979)
7	MAR	22.36 °N, 45.20 °W	Washington 65, St 10, Dr 5, Sm L	(VG 273)
8	MAR	22.36 °N, 45.20 °W	Washington 65, St 10, Dr 5, Sm 9	(VG 921)
9	MAR	22.52 °N, 45.05 °W	Washington 65, St 8, Dr 4, Sm 293	(VG 909)
10	MAR	23.03 °N, 44.91 °W	Atlantis II 92, St 30, Dr 6	(VG 2555)
11	MAR	23.03 °N, 45.03 °W	Atlantis II 92, St 29, Dr 5	(VG 2527)
12	JDF	44.33 °N, 129.92 °W	Oceanographer 68, Dr 5	(VG 180)
13	JDF	44.42 °N, 129.92 °W	Oceanographer 68, Dr 6	(VG 183)
14	MAR	26.06 °N, 44.39 °W	Kurchatov 20	(1A-16)
15	GAL	00.71 °N, 85.50 °W	Desteigeur 41, Dr 1	(VG 1011)
16	GAL	00.71 °N, 85.50 °W	Desteigeur 41, Dr 1	(VG 1009)

TABLE 2

Compositions and liquidus estimated conditions for selected abyssal glasses (localities from Table 1)

	MORB-1						MORB-2								Fe-Ti basalt	
	1	2	3	4	5	6	7	8	9	10	11	12	13	14	15	16
SiO_2	49.34	48.91	51.13	51.15	50.87	50.08	50.44	51.14	50.35	51.27	51.29	50.01	50.18	49.42	49.17	49.87
TiO_2	0.91	0.88	1.23	1.04	1.36	1.16	1.98	1.98	1.72	1.69	1.75	2.74	2.28	1.61	3.69	3.73
Al_2O_3	16.18	16.09	14.89	15.04	14.33	15.80	15.22	15.27	15.43	14.95	15.15	13.31	13.62	15.82	11.14	11.12
Fe_2O_3	1.05	1.65	1.57	1.40	1.79	1.77	2.74	2.76	2.70	2.45	2.12	2.98	2.71	1.90	5.52	5.39
FeO	8.10	7.54	8.21	7.98	9.81	7.79	8.49	8.56	7.62	7.95	8.22	11.99	11.07	7.82	13.53	13.69
MgO	9.36	9.96	7.73	8.19	7.34	7.78	6.76	6.88	7.45	6.96	7.19	5.63	6.12	7.99	4.24	4.29
CaO	12.39	12.26	12.65	13.10	11.56	11.96	10.90	10.99	11.27	11.03	11.15	10.50	11.06	10.98	9.10	9.29
Na_2O	1.93	2.11	2.06	2.03	2.10	2.45	3.12	3.14	2.81	3.05	2.92	2.80	2.72	2.84	2.52	2.50
K_2O	0.13	0.13	0.18	0.10	0.16	0.19	0.14	0.14	0.10	0.13	0.12	0.26	0.16	0.13	0.19	0.19
P_2O_5	0.11	0.10	0.13	0.12		0.13	0.15	0.16	0.13	0.16	0.19	0.22	0.14		0.32	0.30
Total	99.50	99.63	99.78	100.15	99.32	99.11	99.94	101.02	99.58	99.64	100.10	100.44	100.06	98.51	99.42	100.37
(FeO)	9.05	9.02	9.62	9.24	11.42	9.38	10.96	11.04	10.05	10.15	10.13	14.67	13.51	9.53	18.50	18.54
$Fe^{3+}/(Fe^{3+}+Fe^{2+})$ (1)	0.086	0.158	0.141	0.143	0.136	0.169	0.248	0.247	0.247	0.217	0.213	0.183	0.164	0.179	0.262	0.231
(2)	0.125	0.171	0.152	0.130			0.190	0.204	0.236		0.163		0.211		0.275	0.293
(3)	0.103												0.168			
Average	0.105	0.165	0.147	0.137	0.136	0.169	0.219	0.225	0.242	0.217	0.188	0.183	0.181	0.179	0.269	0.262
$Mg/(Mg+Fe^{2+})$	0.673	0.702	0.627	0.647	0.572	0.640	0.587	0.589	0.635	0.610	0.609	0.456	0.496	0.646	0.358	0.358
$T(°C)$	1222	1239	1177	1187	1173	1186	1164	1166	1179	1171	1175	1130	1142	1203	1089	1089
$-\log f_{O_2}$	8.3	7.0	8.3	8.4	8.4	7.8	7.5	7.5	7.1	7.6	7.8	8.6	8.4	7.4	8.2	8.3

to be derived from a primary high-magnesian tholeiite melt with higher Al_2O_3, Na_2O and TiO_2 content, originating from a dry plagioclase lherzolite at $T \sim 1250\,^{\circ}C$ and $P = 5$–9 kbar. The degree of partial melting in both cases appears to be similar (15% and 13%, respectively) [13,16]. The purpose of this article is to determine the oxidation state for MORB-1 and MORB-2 crystallization.

2. Oxygen fugacity

Fourteen samples of fresh abyssal glasses of various compositions were selected from the Smithsonian collections [25] and two samples from the Vernadsky Institute (Tables 1 and 2) in order to determine oxidation states. The oxides were determined by electron microprobe at the Smithsonian Institution and Vernadsky Institute, and the ferrous/ferric ratios were determined at the Vernadsky Institute by Mössbauer spectroscopy with average reproducibility of about $\pm 11\%$ [26]. Variation diagrams (Fig. 2) show the change of glass compositions as a function of Mg-number ($= Mg/(Mg + Fe^{2+})$), and reveal the two main compositional groups mentioned above. The concentrations of Na_2O and TiO_2 are particularly important discriminants for MORB-1 and MORB-2 [1,9,12]. The correlation between Mg-number and Al_2O_3 and TiO_2 reflect the typical tholeiite differentiation trend. A third group lies outside the two main groups and includes only two samples, both titanium-rich ferrobasalts from the Galapagos spreading center.

We find three different levels of iron oxidation state (Fig. 3) which correspond to MORB-1, MORB-2, and titanium-rich ferrobasalt. We also find (Fig. 3) that there is no correlation of iron oxidation state with other oxides within any of the groups. Furthermore, data reported by Bryan et al. [27] on the 13 samples of fresh aphyric basalts from 22–25 °N of the Mid-Atlantic Ridge and from the Kane fracture zone [27] plot tightly within the MORB-2 field (Figs. 2, 3).

The different iron oxidation states cannot be explained by fractionation of high-magnesian olivine and pyroxene from MORB-1 melt to give

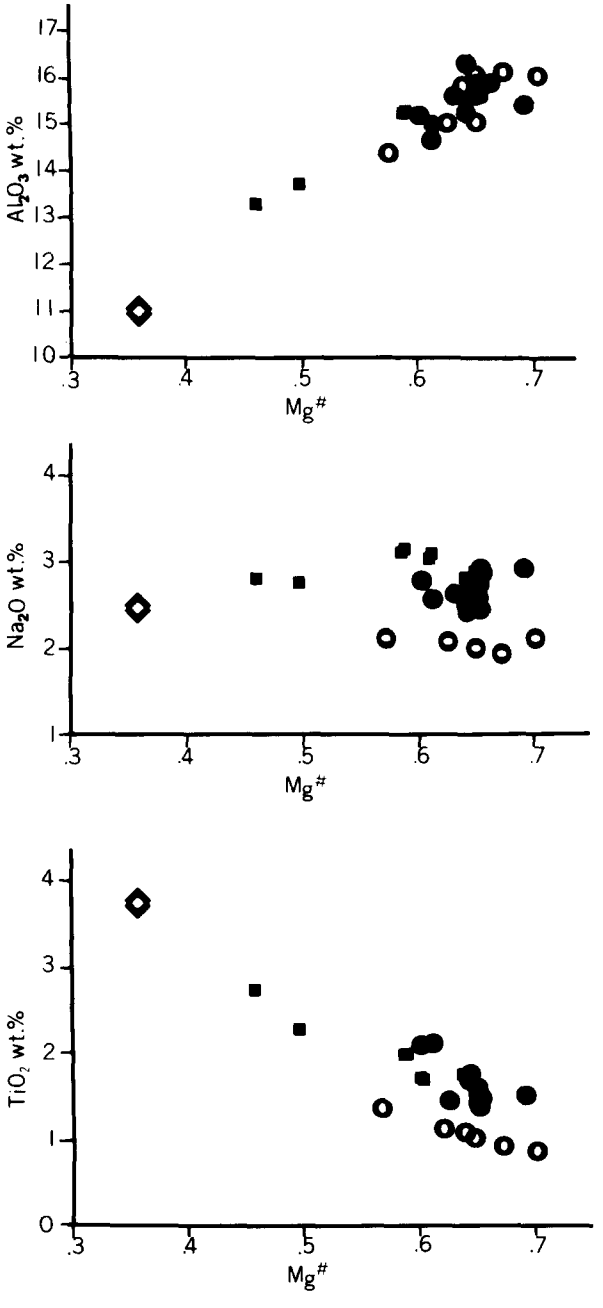

Fig. 2. Variation diagrams for selected abyssal glasses. Mg-number = $Mg/(Mg + Fe^{2+})$. ○ = glass of MORB-1; ■ = glass of MORB-2; ◇ = glass of titanium-rich ferrobasalt; ● = fresh aphyric basalts from 22–25 °N of MAR and from Kane fracture zone [27].

MORB-2 or titanium-rich ferrobasalt melts. Simple calculations show that loss of at least 60% of olivine (Fo_{90}) is required to raise $Fe^{3+}/(Fe^{3+} + Fe^{2+})$ from 0.15 to 0.25. Also, petrography and the differences in other element abundances rule out such fractionation. We thus conclude that the difference in iron oxidation states between MORB-1 and MORB-2 reflects oxygen buffered conditions at their sources.

The liquidus temperatures at 1 atm pressure for glass compositions and for fresh aphyric basalts [27] were calculated from experimental data on olivine-melt equilibria by Ford et al. [28]. Such calculations are based on the Fe-Mg partition

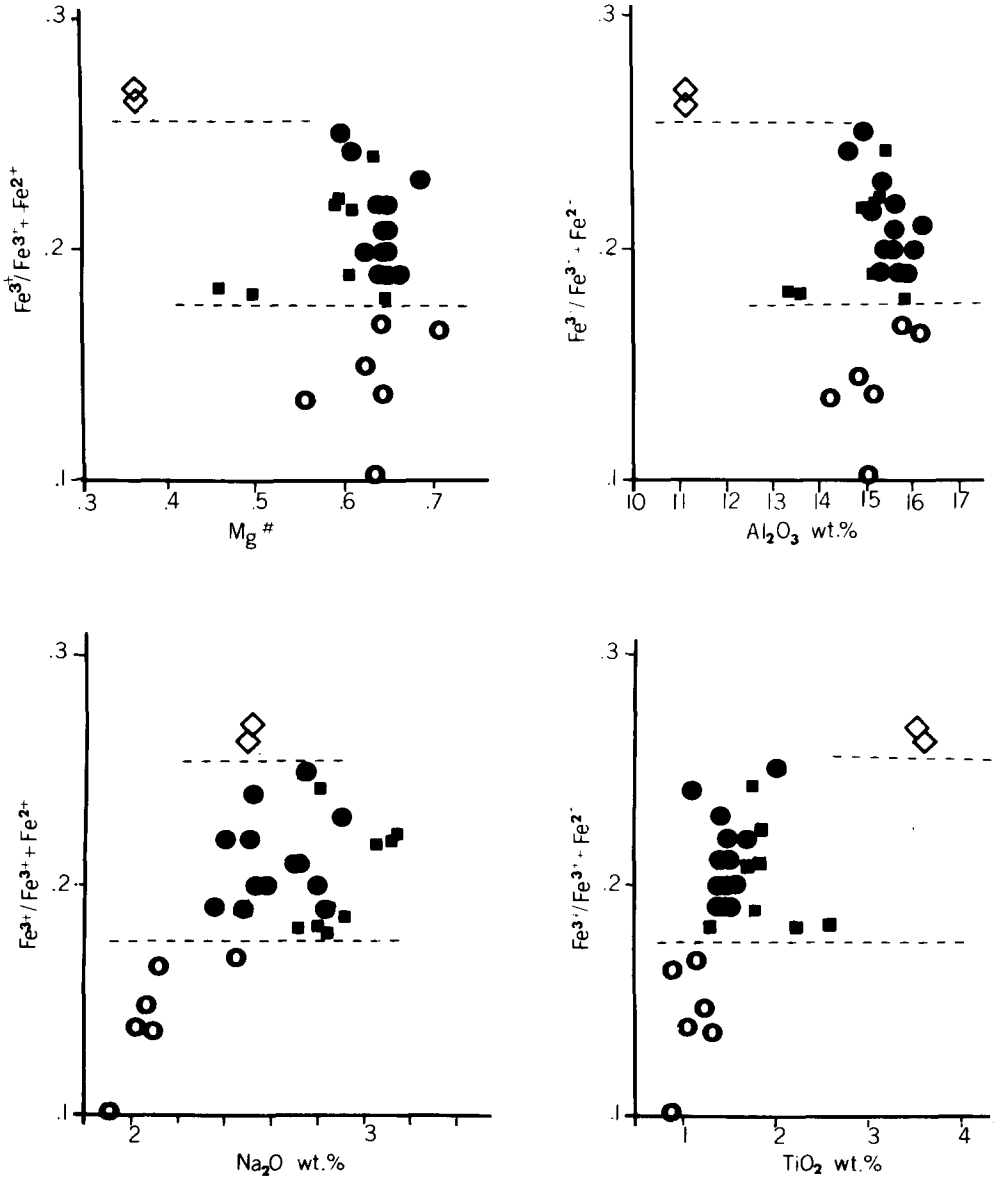

Fig. 3. The different levels of iron oxidation state for selected abyssal glasses and aphyric basalts [27]. For legend see Fig. 2.

coefficients and on the assumption that olivine is one of the liquidus phases for all the glasses studied, an assumption consistent with our observations. The experimentally determined error of such calculations averages $\pm 10\,^{\circ}C$ [28].

Oxygen fugacity is calculated from the empirical equation of Sack et al. [29], which describes the relation between f_{O_2}, composition, degree of iron oxidation, and melt temperature. This equation is based on rather good statistics involving data of 143 melt compositions. However, some systematic errors should be expected ($\sigma \leqslant 0.4$ log units) [29], together with an error of ± 0.3 log units caused by the average standard deviation (11% relative) of $Fe^{3+}/(Fe^{3+} + Fe^{2+})$ ratios. The calculated temperature and oxygen fugacity are shown in Table 2 and in Fig. 4, where the oxygen buffer curves for Ni-NiO (NNO) [30] and quartz-fayalite-magnetite (QFM) [31] are also plotted.

We believe that the degree of iron oxidation does not significantly change during or after glass quenching, and this permits us to discuss the magmatic process in terms of oxygen fugacity calculated from the glasses studied. This position is supported by the correspondence between our data and experimentally estimated f_{O_2}: close to NNO buffer for Leg 46 basalts (MORB-2) [32], between QFM and magnetite-water (MW) buffers for FAMOUS basalts (MORB-1) [33], and a uniform level of $Fe^{3+}/(Fe^{3+} + Fe^{2+})$ ratios for glasses from one locality and from one group. The exception to this is sample VG 3393 (sample 2, Tables 1, 2) which has the same composition as the sample VG 3424 (sample 1, Tables 1, 2) from its neighboring locality but a higher degree of iron oxidation. Moreover, the magmatic origin of the iron oxidation state in aphyric basalts (MORB-2) reported by Bryan et al. [27] is confirmed by reasonable values of $K_{Ol\text{-}liq}^{Fe\text{-}Mg} = 0.26\text{–}0.35$ (for the most part 0.28–0.30) for olivine-basalt pairs [27].

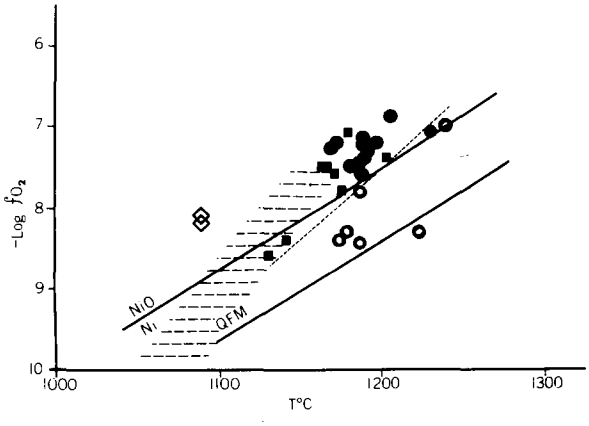

Fig. 4. Temperature-oxygen fugacity plot for selected abyssal glasses and aphyric basalts [27]. Solid lines correspond to NNO and QFM buffers [30,31]. Dashed area shows the high temperature f_{O_2}-T path for the terrestrial basalts after Haggerty [34]. Dashed line separates MORB-1 and MORB-2 f_{O_2}-T conditions. Other symbols see Fig. 2.

Independent data for f_{O_2} of MORB crystallization are available only from near-solidus temperatures ($< 1100\,^{\circ}C$) where ilmenite and magnetite crystallize. Such data [34] show f_{O_2} conditions that are close to the QFM buffer, thus indicating a significantly lower f_{O_2} compared with our high-temperature data on MORB-2 glasses. However, high-temperature f_{O_2} data for ilmenite-magnetite pairs in alkaline basalts [34] are in general agreement with our values and clearly show the reduction trend with decreasing temperature (Fig. 4). The unusually high f_{O_2} estimated for the Fe-Ti Galapagos glasses need to be confirmed by additional data.

In summary, the results reported here in terms of oxidation state regimes confirm the idea of the independent existence of MORB-1 and MORB-2 parental magmas and their derivatives.

Acknowledgements

We are grateful to T. O'Hearn, W. Bryan, D.C. Presnall, and D. Reid Jerez for the critical review of our manuscript and for helpful discussions. We wish to thank T. O'Hearn of the Smithsonian Institution for microprobe analyses, and L. Knapp for drafting the illustrations.

References

1 F. Shido and A. Miyashiro, Compositional difference between abyssal tholeiites from north and south of the Azores on the Mid-Atlantic Ridge, Nature Phys. Sci. 245, 59–60, 1973.

2 H. Bougault and M. Treuil, Mid-Atlantic Ridge: zero-age geochemical variations between Azores and 22° N, Nature 286, 209–212, 1980.
3 H. Bougault, J. Joron and M. Treuil, Alteration, fractional crystallization, partial melting, mantle properties from trace elements in basalts recovered in the North Atlantic, in: Deep Drilling Results in the Atlantic Ocean: Ocean Crust, M. Talwani et al., eds., Ewing Ser. 2, Am. Geophys. Union, M. Ewing Ser. 2, 249–261, 1979.
4 J.G. Schilling, F.M. Zajac, R. Evans, T. Johnston, W. White, J.D. Devine and Kingsley, Petrologic and geochemical variations along the Mid-Atlantic Ridge from 29° N to 73° N, Am. J. Sci. 283, 510–586, 1983.
5 M. Dungan, J. Rhodes and P. Long, The petrology and geochemistry of basalts from Site 396, Legs 45 and 46 of the Deep Sea Drilling Project, in: L. Dmitriev, J. Heirzler et al., Initial Reports of the Deep Sea Drilling Project 46, p. 89, U.S. Government Printing Office, Washington, D.C., 1978.
6 M.F.J. Flower, Accumulation of calcic plagioclase in ocean ridge tholeiite: an indication of spreading rate?, Nature 287, 530–532, 1980.
7 M.F.J. Flower, Thermal and kinematic control on ocean-ridge magma fractionation: contrasts between Atlantic and Pacific spreading axis, J. Geol. Soc. London 138, 695–712, 1981.
8 J.H. Natland, Effect of axial magma chambers beneath spreading centers on the compositions of basaltic rocks, in: B.R. Rosendahl, R. Hekinian et al., Initial Reports of the Deep Sea Drilling Project 54, pp. 833–850, U.S. Government Printing Office, Washington, D.C., 1980.
9 L.V. Dmitriev, A.V. Sobolev and N.M. Suschevskaya, The primary melt of volcanic tholeiite and the oceanic upper mantle composition, Kikl. Akad. Nauk SSSR 240, 177–180, 1978.
10 L.V. Dmitriev, A.V. Sobolev and N.M. Suschevskaya, Conditions of formation of the primary melts of oceanic tholeiites and their compositional variations, Geochimiya 2, 163–177, 1979.
11 L.V. Dmitriev, A.V. Sobolev and N.M. Suschevskaya, The primary melt of the oceanic tholeiite and the upper mantle composition, in: Deep Drilling Results in the Atlantic Ocean: Ocean Crust, M. Talwani et al., eds., Am. Geophys. Union, M. Ewing Ser. 2, 302–313, 1979.
12 W.G. Melson and T. O'Hearn, Basaltic glass erupted along the Mid-Atlantic Ridge between 0-37° N: relationships between composition and latitude, in: Deep Drilling Results in the Atlantic Ocean: Ocean Crust, M. Talwani et al., eds., Am. Geophys. Union, M. Ewing Ser. 2, 249–261, 1979.
13 L.V. Dmitriev, A.V. Sobolev, N.M. Suschevskaya and S.A. Zapunniy, Abyssal glasses, petrological mapping of the oceanic floor and "Geochemical Leg 82", in: Deep Sea Drilling Project 82, U.S. Government Printing Office, Washington, D.C. (in press).
14 N.M. Suschevskaya, L.V. Dmitriev and A.V. Sobolev, Petrochemical criterion for quenched abyssal glasses classification, Dokl. Acad. Nauk USSR 268(6), 1475–1477, 1983.
15 N.M. Suschevskaya, Primary melt of the oceanic tholeiite and variability of basalts from the second seismic layer of the Atlantic Ocean, Ph.D. Thesis, Vernadsky Institute of Geochemistry and Analytical Chemistry, Acad. Sci. USSR Moscow, 1982 (unpublished).
16 L.V. Dmitriev, A.V. Sobolev, N.M. Suschevskaya, W.G. Melson and T. O'Hearn, The evolution of the tholeiite magmatism in world ocean rift zones, 27th Int. Geol. Congr., C.06.1.4, Moscow, 1984 (in press).
17 N.M. Suschevskaya, L.V. Dmitriev, A.I. Almuhamedov, G.M. Kolesov and E. Sherbovsky, Origin and geochemical peculiarities of the Red Sea tholeiitic melts, Geochimiya 7, 1984 (in press).
18 G.M. Biggar, Crystallization of plagioclase, augite, and olivine in synthetic systems and in tholeiites, Mineral. Mag. 47, 161–176, 1983.
19 D.C. Presnall, J.R. Dixon, T.H. O'Donnell and S.A. Dixon, Generation of mid-ocean ridge tholeiites, J. Petrol. 20, 3–35, 1979.
20 A.L. Jaques and D.H. Green, Anhydrous melting of peridotite at 0–15 kb pressure and the genesis of tholeiitic basalts, Contrib. Mineral. Petrol. 73, 287–310, 1980.
21 E. Stolper, Phase diagram for mid-ocean ridge basalts: preliminary results and implications for petrogenesis, Contrib. Mineral. Petrol. 74, 13–27, 1980.
22 T. Fuji and H. Bougault, Melting relations of a magnesian abyssal tholeiite and the origin of MORB's, Earth Planet. Sci. Lett. 62, 283–295, 1983.
23 J.F. Bender, F.N. Hodges and A.E. Bence, Petrogenesis of basalts from the Project FAMOUS area: experimental study from 0 to 15 kbar, Earth Planet. Sci. Lett. 41, 277–302, 1978.
24 S.A. Zapunniy, A.V. Sobolev, A.A. Kadik and L.V. Dmitriev, Crystallization of basalts from the Atlantic ocean: experimental study at 1 atm. under controlled oxygen fugacity, in: IX Conf. Geochemistry of Magmatic Rocks, Moscow, Abstr., pp. 20–21, 1983.
25 W.G. Melson, G.R. Byerly, J.A. Nelen, T.O'Hearn, T.L. Wright and T. Vallier, A catalog of the major element chemistry of abyssal volcanic glasses, Mineral Sci. Inv. 1974-1975, Smithson. Contrib. Earth Sci. 19, 31–60, 1977.
26 T.V. Malysheva, Mössbauer Effect in Geochemistry and Cosmochemistry, Nauka, Moscow, 1975.
27 W.B. Bryan, G. Thompson and J.N. Ludden, Compositional variation in normal MORB from 22°–25° N Mid-Atlantic Ridge and Kane fracture zone, J. Geophys. Res. 86, 11815–11836, 1981.
28 C.E. Ford, D.G. Russell, J.A. Craven and M.R. Fisk, Olivine-liquid equilibria: temperature, pressure and composition dependence of the crystal/liquid cation partition coefficients for Mg, Fe^{2+}, Ca, and Mn, J. Petrol. 24, 256–265, 1983.
29 R.O. Sack, I.S.E. Carmichael, M. Rivers and M.S. Ghiorso, Ferric-ferrous equilibria in natural silicate liquids at 1 bar, Contrib. Mineral. Petrol. 75, 369–376, 1980.
30 J.S. Huebner and M. Sato, The oxygen fugacity-temperature relationships of manganese oxide and nickel oxide buffers, Am. Mineral. 55, 934–952, 1970.

31 R.J. Williams, Reaction constants in the system Fe-MgO-SiO_2-O_2 at 1 atm. between 900 °C and 1300 °C: experimental results, Am. J. Sci. 270, 334–360, 1971.
32 H. Fukuyama and K. Hamuro, Melting relations of Leg 46 basalts at atmospheric pressure, in: L. Dmitriev, J. Heirzler et al., Initial Reports of the Deep Sea Drilling Project 46, pp. 235–239, U.S. Government Printing Office, Washington, D.C., 1978.
33 M.R. Fisk and A.E. Bence, Experimental crystallization of chrome spinel in FAMOUS basalt 527-1-1, Earth Planet. Sci. Lett. 48, 111–123, 1978.
34 S.E. Haggerty, The redox state of planetary basalts, Geophys. Res. Lett. 5, 443–446, 1978.